# Ten-fold Enhancement of InAs Nanowire Photoluminescence Emission with an InP Passivation Layer

## Table of Content

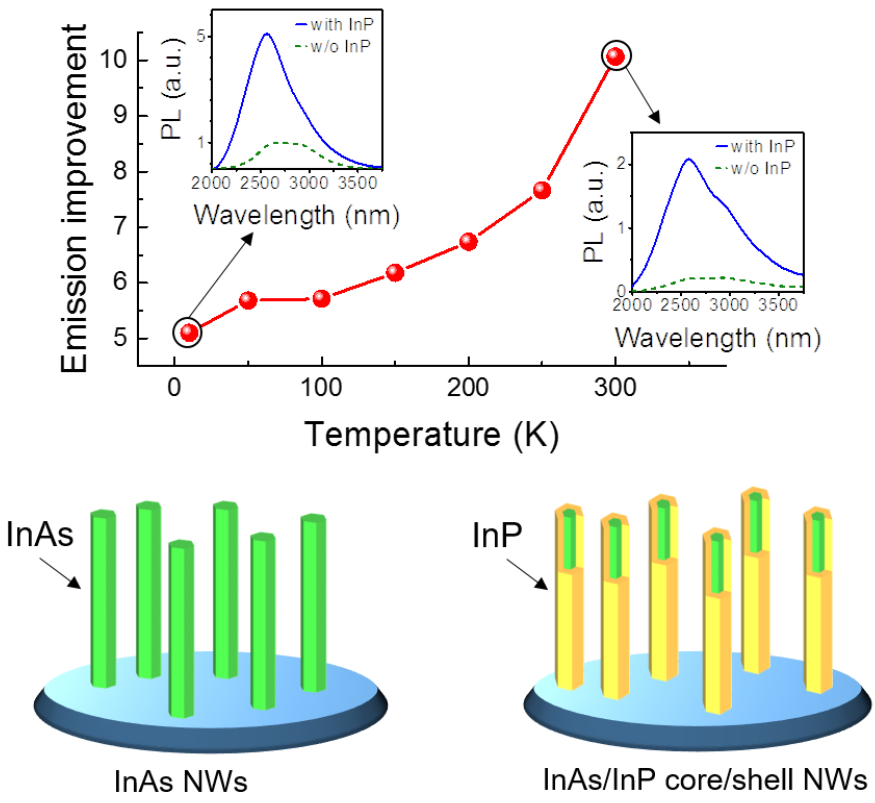

# Ten-fold Enhancement of InAs Nanowire Photoluminescence Emission with an InP Passivation Layer

*Pamela Jurczak,*[†‡] Yunyan Zhang,*[†‡] Jiang Wu,*[†] Ana M. Sanchez,[‡] Martin Aagesen,[#] and Huiyun Liu[†]*

[†]Department of Electronic and Electrical Engineering, University College London, London WC1E 7JE, United Kingdom

[‡]Department of Physics, University of Warwick, Coventry CV4 7AL, United Kingdom

[#]Center for Quantum Devices, Niels Bohr Institute, University of Copenhagen, Universitetsparken 5, 2100 Copenhagen, Denmark

**ABSTRACT**: In this letter, we demonstrate that a significant improvement of optical performance of InAs nanowires can be achieved by capping the core InAs nanowires with a thin InP shell, which successfully passivates the surface states reducing the rate of non-radiative recombination. The improvements have been confirmed by detailed photoluminescence measurements, which showed up to ten-fold increase in the intensity of room-temperature photoluminescence from the capped InAs/InP nanowires compared to the sample with core-only InAs nanowires. Moreover, the nanowires exhibit high stability of total photoluminescence emission strength across temperature range from 10 to 300 K as a result of strong quantum confinement. These findings could be the key to successful implementation of InAs nanowires into optoelectronic devices.

**KEYWORDS**: Nanowires, InAs, self-catalyzed, photoluminescence

InAs is considered to be one of the most suitable semiconductors for mid-wave infrared (mid-IR) devices such as lasers or detectors due to its narrow, direct bandgap and high electron mobility.[1] Combination of these material properties and unique 1D structure of nanowires (NWs) enables creation of a new generation of nanoscale photonic and optoelectronic devices using InAs nanowires as building blocks.[2] Due to their superb electronic properties and strong quantum confinement effects, they are also highly suitable for a large range of other applications such as transistors,[3-7] p-n junctions,[4,8] high-performance nanoelectronics,[9,10] logical elements,[11] single electron circuits,[2,12-15] spintronic[16] and quantum electronic devices.[2,16-20]

NWs have significant advantages over thin films and bulk materials due to their small dimensions: diameter of up to few hundred nanometers and length of several microns.[21,22] They can be integrated on a large variety of substrates such as silicon or organic polymers,[23-25] because their small contact area with the substrate confines the strain relaxation-formed dislocations to the NW/substrate interface. This means great flexibility in device design, potential for low cost fabrication and seamless integration with silicon industrial platform. The small dimensions can also result in quantum confinement of carriers.[26] Geometry of the NWs is especially beneficial for photovoltaic and detector applications due to their low reflectivity and enhanced absorption.[27-29] It also provides an efficient path for charge separation and carrier extraction crucial for robust operation of photovoltaic devices.

The main challenge in producing high-performance InAs NWs-based optoelectronic and photonic devices is that good optical properties are hard to achieve. This is caused by poor material quality and high levels of surface states emission due to large surface-to-volume ratio of NWs and defect states near surfaces.[30] While high surface electron density of InAs is a desirable characteristic for electronic devices due to ease of ohmic contact formation, it hinders the optical performance. Due

to this roadblock, most studies so far focused on electrical properties of the InAs nanowires[7,31,32] and fabrication of electronic and quantum devices. Only recently some low temperature optical studies have been reported,[26,33-35] but the signal quality is low due to high numbers of defects and impurities.

We have identified two key factors required to achieve strong emission from the nanowires and hence obtain high quality devices: improved material quality and suppression of surface states. High-quality InAs nanowires have been demonstrated by using Au catalyst particles,[2,9,33,34,36,37-41] but these are not compatible with complementary metal-oxide-semiconductor (CMOS) industrial standards. Therefore, a self-catalysed growth method is more suitable. However, it requires fine levels of control in order to successfully produce high quality material. This level of precision can be achieved using molecular beam epitaxy (MBE), where the high-vacuum environment also helps in reducing incorporation of impurities. Elimination of surface states can be achieved by passivation of the NWs using a thin coating layer of other, less susceptible material.

In this work, we investigate the effects of using an ultra-thin InP capping layer on optical properties of the InAs NWs. For this purpose, two samples have been grown and analyzed: core-only InAs NWs and InAs/InP core/shell NWs. We demonstrate successful surface passivation and hence an up to ten-fold improvement in photoluminescence emission. Moreover, good temperature stability and high carrier confinement has been observed for both samples, which lead to strong emission even at room temperature. This work overcomes a major roadblock of poor optical properties from InAs NWs, and hence could potentially enable successful realization of InAs NW photonic and optoelectronic devices.

The nanowires have been grown by a solid-source Veeco Gen930 molecular beam epitaxy (MBE) system with solid In source and $As_4$ and $P_2$ cracker cells. The self-catalyzed InAs NWs were grown

directly on p-type Si(111) substrate at an In flux, V/III ratio, temperature and growth duration of $4.78\times10^{-8}$ Torr, 288, 450$^0$C and 1 hour, respectively. The InP shell was grown at an In flux, V/III ratio, temperature and growth duration of $4.78\times10^{-8}$ Torr, 60, 400$^0$C and 10 minutes, respectively.

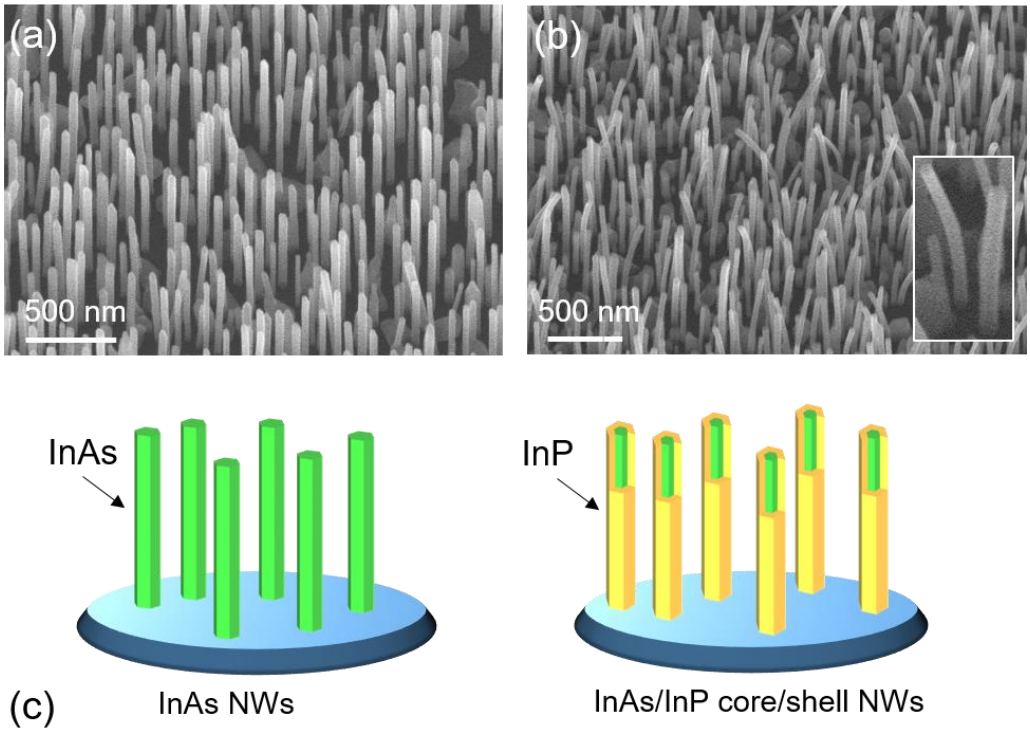


**Figure 1.** SEM images (tilt angle 25$^0$) of (a) InAs core-only NWs and (b) InAs/InP core/shell NWs grown on Si(111) substrates via a self-catalyzed MBE growth method. The inset in (b) shows a high magnification image of single InAs/InP nanowires. (c) Illustration of InAs core-only NWs and InAs/InP core/shell NWs.

Figures 1a and 1b show tilted view (25$^0$) of InAs core-only NWs and InAs/InP core/shell NWs, respectively. The nanowires have been grown vertically on the silicon substrate. The schematics of the NWs are shown in Fig. 1c. They are of good overall quality and are uniform in diameter, density and length. For both samples the NWs are about 500 nm long with diameters of 55-60 nm, 3-5 nm of which in InAs/InP nanowires account for the shell (shell thickness determined by TEM, Fig. 2(a)). There is a noticeable difference in the shape of the nanowires. While the core-only NWs

are perfectly straight, the core/shell ones are visibly bent, which is caused by stress induced on the core of the nanowire by the shell. [42]

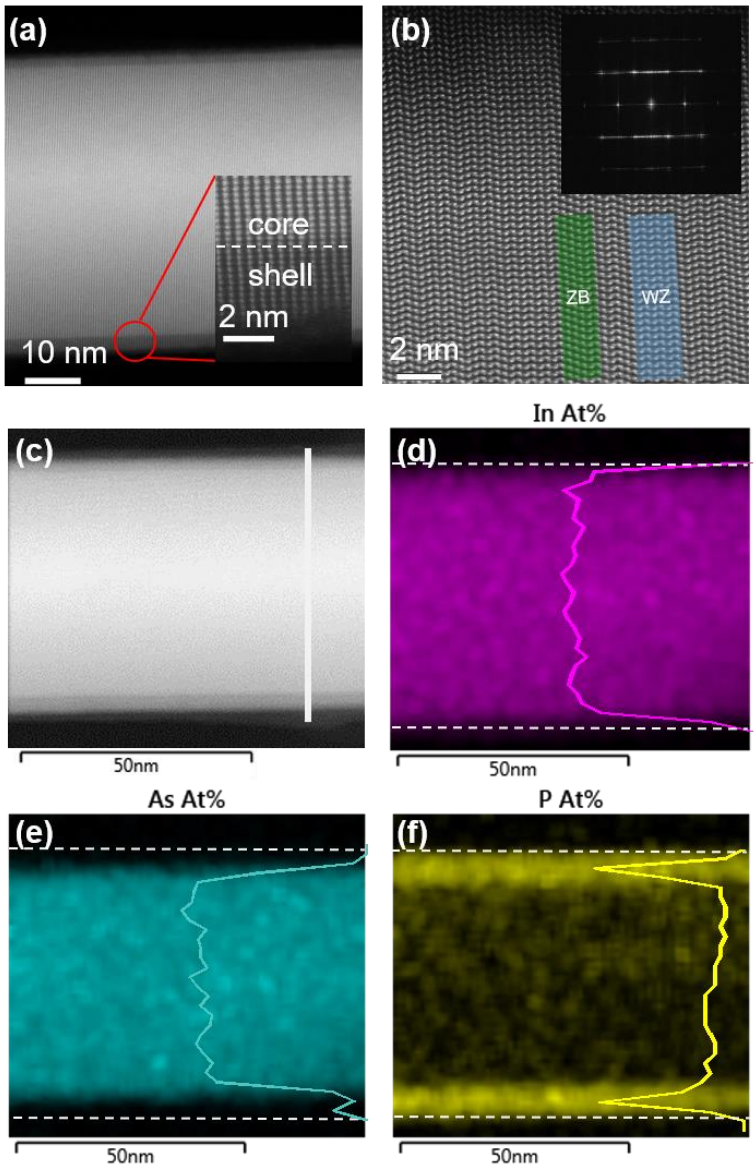


**Figure 2.** (a) <112> ADF-STEM image of a middle section of one of the InAs/InP NWs clearly showing the core and shell parts of the structure. (b) <110> ADF-STEM image of a middle section of one of the InAs/InP NWs showing polytypic structure of the nanowires with highlighted examples of wurtzite (blue) and zinc-blende (green) crystal phases. The inset shows the selective area electron diffraction pattern taken for one of the nanowires confirming that both wurtzite (WZ) and zinc-blende (ZB) phases are present. Analysis of the composition of the InAs/InP NWs with EDX. (c) Middle section of a NW with highlighted (d) In, (e) As and (f) P elemental distribution as a percentage of all the elements in the nanowire (at%). EDX line profile taken along the white

line indicated in (c) corresponding to the In, As and P have also been plotted in (d), (e) and (f), respectively.

The ADF-STEM images of the InAs/InP sample have been taken using a doubly aberration corrected ARM 200 microscope. Figure 2a confirms presence of a thin, around 3 nm thick shell with different composition than the core. No defects have been observed at the interface between the InAs core and the InP shell. The ADF-STEM image in Figure 2b shows atomic stacking within the InAs/InP nanowire. A polytypic structure of the nanowires is clearly revealed with highlighted examples of WZ (blue) and ZB (green) crystal phases. Both phases are present and it has also been confirmed by the selective area electron diffraction pattern (Figure 2b inset). The composition switches between the two phases depending on fluctuations of growth temperature and flux ratios. Further work on the growth conditions is required in order to fine tune these parameters and obtain pure-phase InAs NWs.

Figure 2c-f shows the results of composition analysis of the InAs/InP NWs performed with energy-dispersive x-ray spectroscopy (EDS). Fragment of a middle section of a nanowire, shown in Figure 2c, has been analyzed and showed uniform distribution of indium throughout the sample (Figure 2d) and arsenic (Figure 2e) within the core. Figure 2f shows high phosphorus content within the thin shell of the nanowire. However, the InAs/InP interface is not abrupt and some intermixing of P with As occurs in the InAs atomic layers close to the shell. The line plots in Figure 2d-f show concentrations of In, As and P atoms along the cross section of a middle part of the NW indicated with the line in Figure 2c. This confirms the composition of the core as InAs and the shell as InP.

A mid-IR PL setup has been used to analyze the photoluminescence properties of both samples. A 532 nm laser has been used to illuminate the samples and a liquid nitrogen cooled InSb detector to record the photoluminescence of the samples. In order to ensure that the collected signal originated

from the nanowires, prior to the measurements they have been mechanically removed from the as-grown sample (via ultrasonication) and placed on a clean piece of silicon substrate. During the deposition process, certain steps were taken to make sure the densities are comparable. The samples were placed in a closed-cycle liquid helium cooled cryostat kept under vacuum. The measurements have been taken at a range of temperatures between 10 and 300 K. For power-dependent measurements laser powers between 50 and 600 mW have been used, where the power delivered to the sample is half of the laser output. For temperature-dependent measurements laser power of 600 mW (300 mW at the sample) has been used.

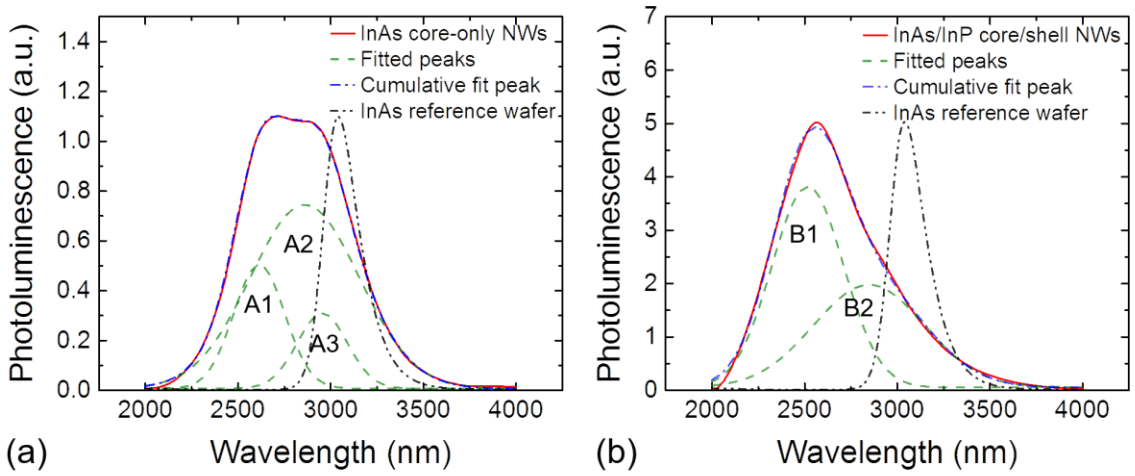


**Figure 3.** PL spectra taken at 10K for (a) the InAs core-only and (b) the InAs/InP core/shell nanowires with InAs wafer emission as reference. Measured signal (red), fitted Gaussian peaks (green), sum of the fitted peaks (blue) and normalized InAs wafer reference (black) have been plotted.

Figure 3a shows PL spectrum of the InAs nanowires taken at 10 K. The spectrum can be resolved into three peaks, A1 centered around 2607 nm (475.6 meV), A2 at 2835 nm (437.3 meV) and A3 at 2932 nm (422.9 meV). Figure 4b shows that only two peaks are present in the PL spectrum of the InAs/InP nanowires, B1 at 2524 nm (491.2 meV) and B2 at 2833 nm (437.6 meV). All of the

peaks observed in Figures 3a and 3b are blue-shifted from the bulk InAs emission (around 3000 nm, 415 meV from literature;[43] 3026 nm, 409.7 meV from measurement of InAs (ZB) wafer, reference peaks in Figure 3a and 3b). This is most probably caused by size-induced quantization effects or Burstein-Moss (band-filling) effect commonly observed for nanowires.[44] There is also a slight blue shift of the InAs/InP PL peaks compared to core-only InAs due to strain induced by the InP cladding.[45,46] The energy difference between peaks B1 and B2 is 53.6 meV, which is very close to the theoretically predicted difference between bandgaps of wurtzite and zinc blende phases in InAs bulk by Zanolli et al.[47] The energy difference between peaks A1 and A3 can be calculated to equal 52.7 meV, also very close to the theoretical prediction. These observations lead us to believe that peaks A1 and B1 arise from the WZ segments of the nanowires, while peaks A3 and B2 arise from the ZB segments. Due to small diameter of the NWs and high surface electron density in InAs, surface effects dominate recombination processes in InAs NWs. The InP shell passivates the surface and hence suppresses the surface emission in favor of emission from the NW core. Hence peak A2, which is dominant in intensity for the InAs core-only sample, can be attributed to surface states related emission while an analogous peak is not present in the passivated InAs/InP sample.

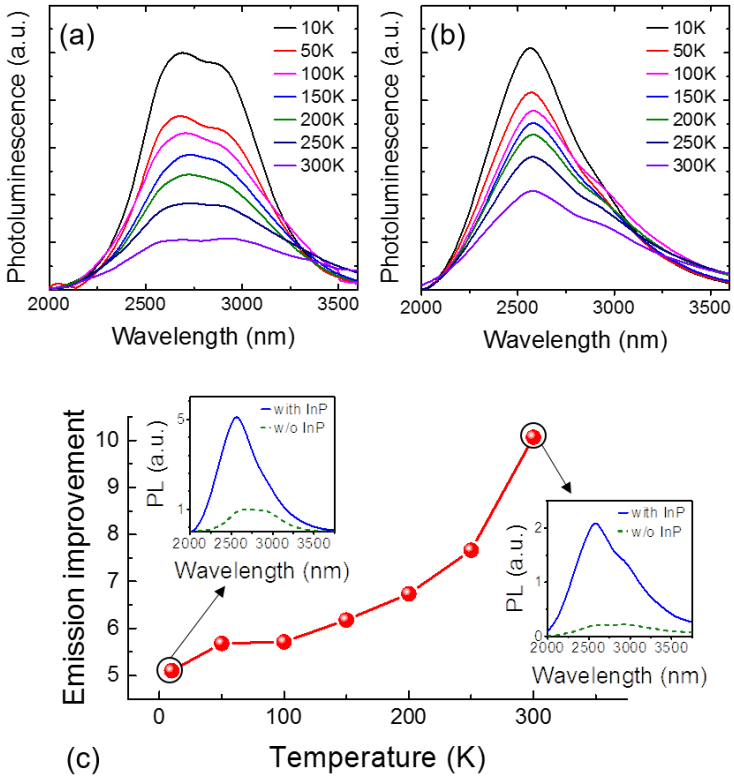


**Figure 4.** PL spectra taken at temperatures between 10 and 300 K for (a) the InAs core-only and (b) the InAs/InP core/shell nanowires. (c) Emission improvement of the InAs/InP NWs over InAs NWs, the insets show PL emission for the two samples at 10 and 300 K.

Figure 4 shows the PL spectra taken for both samples at temperatures between 10 and 300 K. The general shape of the spectra does not change with temperature for the InAs/InP sample (Figure 4b) and the intensity drops with increasing temperature as expected. For the InAs sample (Figure 4a) the relative intensities of the peaks in the spectra change at sample temperatures of 200 K and above. This is due to increased surface states emission relative to the nanowires emission as the surface related processes are more significant at higher temperatures. Strong emission can be observed all the way up to room temperature (300 K), where the intensities of InAs and InAs/InP samples are about 20% and 40% of that at 10 K, respectively. Achieving strong room temperature emission from these nanowires confirms high quality of the material and indicates that it is possible to fabricate InAs NWs-based photonic devices capable of operating at room conditions in near

future. Figure 4c shows the emission improvement of the InP-capped NWs compared to the InAs core-only NWs calculated as a ratio of the maximum peak intensities of the two samples. The ratio increases with the temperature as the InAs NWs are more strongly affected by the thermal effects due to their unpassivated surfaces, which once again confirms the effectiveness of the InP capping layer. At 10 K the overall strength of PL emission from the InAs/InP core/shell NWs is about five times stronger, while at room temperature we observe a ten-fold improvement.

Figure 5 presents results for integrated PL values as function of excitation power and temperature. In Figure 5a a typical trend can be observed for the InAs/InP NWs sample where the integrated PL values rise quickly with increasing power at low powers (up to around 100 mW), and then starts to saturate at higher powers. The shapes of these plots do not change between different sample temperatures, only the overall strength drops as expected based on temperature-dependent PL measurements. For the InAs core-only sample the general trends of the plots are similar to those for InAs/InP, however the saturation point moves towards higher excitation powers as the temperature is increased. These results show that thermally excited recombination processes become more severe as the sample warms up and suggest that the surface states are responsible. Comparing the plots for the two samples it can be observed that the improvement achieved by addition of InP passivation layer is substantial in terms of PL output of the samples.

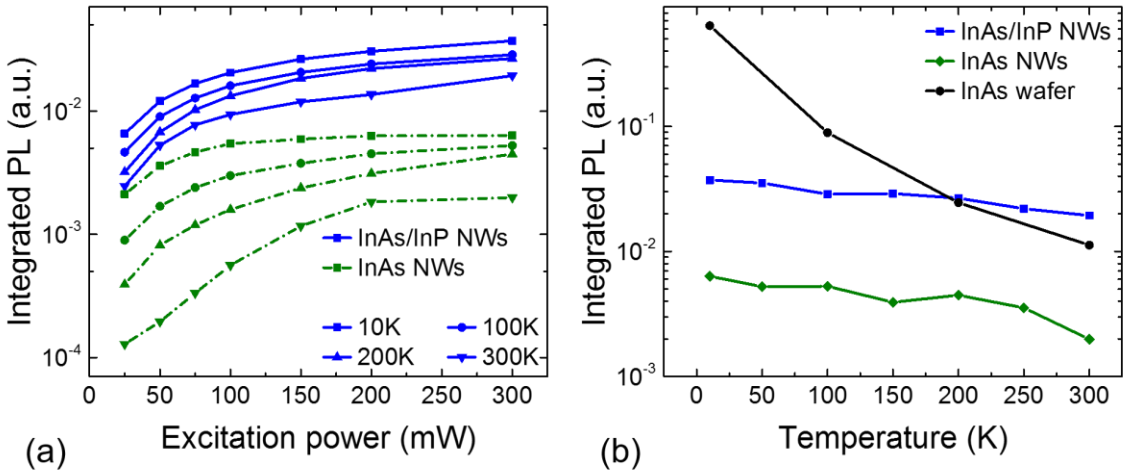


**Figure 5.** Integrated PL as a function of (a) excitation power for a range of temperatures between 10 and 300 K and (b) sample temperature for InAs/InP nanowires (blue), InAs core-only nanowires (green) and InAs wafer (black).

Figure 5b shows how the integrated PL values behave in terms of sample temperature. A usual trend is observed for the InAs wafer, where the integrated PL strength drops rapidly as the temperature is increased by more than order of magnitude between 10 K and room temperature. Both nanowire samples however show remarkable stability across the whole range of temperatures. The integrated PL intensity for the InAs/InP (InAs) sample between 10 and 300 K drops only by a factor of 2 (3). We attribute this behavior to very high carrier confinement within the nanowires. Because of small dimensions of each of the nanowires and small contact area with the substrate, the thermally excited carriers cannot easily escape and then non-radiatively recombine as it happens in bulk materials. The fact that similar trends are observed for both nanowire samples indicate that the effects of confinement are much stronger than any negative influence of surface states. It is also interesting to notice that at temperatures above 200 K the integrated PL of InAs/InP NW sample is higher than that of the InAs wafer. This could be explained by the geometry of the wafer (bulk material) and that it is not passivated.

In conclusion, the effects of InP capping on the optical emission of InAs NWs have been investigated. Effective surface passivation resulted in up to ten-fold improvement of photoluminescence emission from the nanowires when compared to the core-only sample. We presented the first demonstration of room-temperature PL emission from InAs nanowires. Moreover, high carrier confinement within these nanowires can be an important advantage in design of novel electronic and quantum devices or lead to new observations of nanoscale physical phenomena. The results presented here could a high impact on the development of InAs NWs optoelectronic materials and devices.

## AUTHOR INFORMATION

### Corresponding Author

* pamela.jurczak.10@ucl.ac.uk, * yunyan.zhang.11@ucl.ac.uk, * jiang.wu@ucl.ac.uk

### Author Contributions

The manuscript was written through contributions of all authors. All authors have given approval to the final version of the manuscript. ‡These authors contributed equally.

### Notes

The authors declare no competing financial interests.

## ACKNOWLEDGMENT

The authors acknowledge financial support from UK EPSRC under Grants No. EP/P000886/1 and No. EP/P000916/1 and Leverhulme Trust.

## REFERENCES

[1] – Milnes, A.G.; Polyakov, A.Y. *Mat. Sci. Eng. B* **1993**, 18, 237-259

[2] – Fasth, C.; Fuhrer, A.; Samuelson, L.; Golovach, V.N.; Loss, D. *Phys. Rev. Lett.* **2007**, 98, 266801

[3] – Goldberger, J.; Sirbuly, D.J.; Law, M.; Yang, P. *J. Phys. Chem. B* **2004**, 109, 9-14

[4] – Greytak, A.B.; Lauhon, L.J.; Gudiksen, M.S.; Lieber, C.M. *Appl. Phys. Lett.* **2004**, 84, 21

[5] – Cui, Y.; Lieber, C.M. *Science* **2001**, 291, 5505, 851-853

[6] – Ghalamestani, S.G.; Johansson, S.; Borg, B.M.; Lind, E.; Dick, K.A.; Wernersson, L.E. *Nanotechnology* **2012**, 23, 015302

[7] – Tanaka, T.; Tomioka, K.; Hara, S.; Motohisa, J.; Sano, E.; Fukui, T. *Appl. Phys. Express* **2010**, 3, 025003

[8] – Haraguchi, K.; Katsuyama, T.; Hiruma, K.; Ogawa, K. *Appl. Phys. Lett.* **1991**, 60, 106556

[9] – Thelander, C.; Bjork, M.T.; Larsson, M.W.; Hansen, A.E.; Wallenberg, L.R.; Samuelson, L. *Solid State Comm.* **2004**, 131, 573-579

[10] – Jiang, X.; Xiong, Q.; Nam, S.; Qian, F.; Li, Y.; Lieber, C.M. *Nano Lett.* **2007**, 7, 3214-3218

[11] – Huang, Y.; Duan, X.; Cui, Y.; Lauhon, L.J.; Kim, K.H.; Lieber, C.M. *Science* **2001**, 294, 5545

[12] – Zhong, Z.; Fang, Y.; Lu, W.; Lieber, C.M. *Nano Lett.* **2005**, 5, 1143-1146

[13] – Thelander, C.; Martensson, T.; Bjork, M.T.; Ohlsson, B.J.; Larsson, M.W.; Wallenberg, L.R.; Samuelson, L. *Appl. Phys. Lett.* **2003**, 83, 10

[14] – Bjork, M.T.; Thelander, C.; Hansen, A.E.; Jensen, L.E.; Larsson, M.W.; Wallenberg, L.R.; Samuelson, L. *Nano Lett.* **2004**, 4, 1621-1625

[15] – De Franceschi, S.; van Dam, J.A.; Bakkers, E.P.A.M.; Feiner, L.F.; Gurevich, L.; Kouwenhoven, L.P. *Appl. Phys. Lett.* **2003**, 83, 2

[16] – Bjork, M.T.; Fuhrer, A.; Hansen, A.E.; Larsson, M.W.; Froberg, L.E.; Samuelson, L. *Phys. Rev. B* **2005**, 72, 201307

[17] – Kang, J.H.; Ronen, Y.; Cohen, Y.; Convertino, D.; Rossi, A.; Coletti, C.; Heun, S.; Sorba, L.; Kacman, P.; Shtrikman, H. *Semicond. Sci. Technol.* **2016**, 31, 115005

[18] – Loss, D.; DiVincenzo, D.P. *Phys. Rev. A* **1998**, 57,120

[19] – Burkard, G.; Loss, D.; DiVincenzo, D.P. *Phys. Rev. B* **1999**, 59, 2070

[20] – Lu, Wei; Lieber, C.M. *J. Phys. D Appl. Phys.* **2006**, 39, R387

[21] – Hu, Y.; Churchill, H.O.H.; Reilly, D.J.; Xiang, J.; Lieber, C.M.; Marcus, C.M. *Nature Nanotechnology* **2007**, 2, 622-625

[22] – Zhang, Y.; Wu, J.; Aagesen, M.; Liu, H. *J. Phys. D Appl. Phys.* **2015**, 48, 463001

[23] – Zhang, Y.; Aagesen, M.; Holm, J.V.; Jorgensen, H.I.; Wu, J.; Liu, H. *Nano Lett.* **2013**, 13, 3897-3902

[24] – Matteini, F.; Tutuncuoglu, G.; Ruffer, D.; Alarcon-Llado, E.; Fontcuberta i Morral, A. *J. Crys. Growth* **2014**, 404, 246-255

[25] – Klein, L.; Mastrogiovanni, D.; Wan, A.; Garfunkel, E. *InTech* **2011**, Chapter 16

[26] – Koblmuller, G.; Vizbaras, K.; Hertenberger, S.; Bolte, S.; Rudolph, D.; Becker, J.; Doblinger, M.; Amann, M.C.; Finley, J.J.; Abstreiter, G. *Appl. Phys. Lett.* **2012**, 101, 5

[27] – Yablonovitch, E.; Cody, G.D. *IEEE T. Electron. Dev.* **1982**, 29, 300-305

[28] – Krogstrup, P.; Jorgensen, H.I.; Heiss, M.; Demichel, O.; Holm, J.V.; Aagesen, M.; Nygard, J.; Fontcuberta i Morral, A. *Nature Photonics* **2013**, 7, 306-310

[29] – Yablonovitch, E. *J.Opt. Soc. Am.* **1982**, 72, 899-907

[30] – Lu, A.; Zhao, C.; Wu, J. *J. Nanosc. Nanotech.* **2016**, 16, 8146-8149

[31] – Ford, A.C.; Ho, J.C.; Chueh, Y.L.; Tseng, Y.C.; Fan, Z.; Guo, J.; Bokor, J.; Javey, A. *Nano Lett.* **2009**, 9, 360-365

[32] – Wei, W.; Bao, X.Y.; Soci, C.; Ding, Y.; Wang, Z.L.; Wang, D. *Nano Lett.* **2009**, 9, 2926-2934

[33] – Sun, M.H.; Leong, E.S.P.; Chin, A.H.; Ning, C.Z.; Cirlin, G.E.; Samsonenko, Y.B.; Dubrovskii, V.G.; Chuang, L.; Chang-Hasnain, C. *Nanotechnology* **2010**, 21, 33

[34] – Rota, M.B.; Ameruddin, A.S.; Fonseka, H.A.; Gao, Q.; Mura, F.; Polimeni, A.; Miriametro, A.; Tan, H.H.; Jagadish, C.; Capizzi, M. *Nano Lett.* **2016**, 16, 5197-5203

[35] – Hormann, N.G.; Zardo, I.; Hertenberger, S.; Funk, S.; Bolte, S.; Doblinger, M.; Koblmuller, G.; Abstreiter, G. *Phys. Rev. B* **2011**, 84, 155301

[36] – Dubrovskii, V.G.; Sibirev, N.V.; Berdnikov, Y.; Gomes, U.P.; Ercolani, D.; Zannier, V.; Sorba, L. *Nanotechnology* **2016**, 27, 375602

[37] – Dick, K.A.; Thelander, C.; Samuelson, L.; Caroff, P. *Nano Lett.* **2010**, 10, 3494-3499

[38] – Caroff, P.; Dick, K.A.; Johansson, J.; Messing, M.E.; Deppert, K.; Samuelson, L. *Nature Nanotechnology* **2009**, 4, 50-55

[39] – Chuang, L.C.; Moewe, M.; Chase, C.; Kobayashi, N.P.; Chang-Hasnain, C.; Crankshaw, S. *Appl. Phys. Lett.* **2007**, 90, 4

[40] – Roest, A.L.; Verheijen, M.A.; Wunnicke, O.; Serafin, S.; Wondergem, H.; Bakkers, E.P.A.M. *Nanotechnology* **2006**, 17, S271

[41] – Tchernycheva, M.; Travers, L.; Patriarche, G.; Glas, F.; Harmand, J.C.; Cirlin, G.E.; Dubrovskii, V.G. *J. Appl. Phys.* **2007**, 102, 9

[42] – Lin, H.M.; Chen, Y.L.; Yang, J.; Liu, Y.C.; Yin, K.M.; Kai, J.J.; Chen, F.R.; Chen, L.C.; Chen, Y.F.; Chen, C.C. *Nano Lett.* **2003**, 3, 537-541

[43] – InAs band structure and carrier concentration, IOFFE institute, accessed on 3rd February 2017, http://www.ioffe.ru/SVA/NSM/Semicond/InAs/bandstr.html

[44] – Yan, Y.; Liao, Z.M.; Bie, Y.Q.; Wu, H.C.; Zhou, Y.B. *Appl. Phys. Lett.* **2011**, 99, 10

[45] – Shiri, D.; Kong, Y.; Buin, A.; Anantram, M.P. *Appl. Phys. Lett.* **2008**, 93, 7

[46] – Wei, B.; Zheng, K.; Ji, Y.; Zhang, Y.; Zhang, Z.; Han, X. *Nano Lett.* **2012**, 12, 4595-4599

[47] – Zanolli, Z.; Fuchs, F.; Furthmuller, J.; von Barth, U.; Bechstedt, F. *Phys. Rev. B* **2007**, 75, 245121